


# Ultra-low noise and high bandwidth bipolar current driver for precise magnetic field control

Cite as: Rev. Sci. Instrum. **90**, 014701 (2019); <https://doi.org/10.1063/1.5046484>

Submitted: 28 June 2018 . Accepted: 10 December 2018 . Published Online: 02 January 2019

Yu-Meng Yang, Hong-Tai Xie , Wen-Chao Ji, Yue-Fei Wang, Wei-Yong Zhang, Shuai Chen , and Xiao Jiang 



View Online



Export Citation



CrossMark

## ARTICLES YOU MAY BE INTERESTED IN

[A single-chip integrated transceiver for high field NMR magnetometry](#)

Review of Scientific Instruments **90**, 015001 (2019); <https://doi.org/10.1063/1.5066436>

[Contributed Review: A review of compact interferometers](#)

Review of Scientific Instruments **89**, 121501 (2018); <https://doi.org/10.1063/1.5052042>

[Pure sinusoidal photo-modulation using an acousto-optic modulator](#)

Review of Scientific Instruments **89**, 123102 (2018); <https://doi.org/10.1063/1.5020796>



# Ultra-low noise and high bandwidth bipolar current driver for precise magnetic field control

Cite as: Rev. Sci. Instrum. 90, 014701 (2019); doi: 10.1063/1.5046484

Submitted: 28 June 2018 • Accepted: 10 December 2018 •

Published Online: 2 January 2019






View Online



Export Citation



CrossMark

Yu-Meng Yang,<sup>1,2</sup> Hong-Tai Xie,<sup>2,3</sup>  Wen-Chao Ji,<sup>1,2</sup> Yue-Fei Wang,<sup>1,2</sup> Wei-Yong Zhang,<sup>1,2</sup> Shuai Chen,<sup>2,3</sup>   
and Xiao Jiang<sup>1,2,a)</sup> 

## AFFILIATIONS

<sup>1</sup>Hefei National Laboratory for Physical Sciences at the Microscale and Department of Modern Physics, University of Science and Technology of China, Hefei, Anhui 230026, China

<sup>2</sup>CAS Center for Excellence and Synergetic Innovation Center in Quantum Information and Quantum Physics, University of Science and Technology of China, Hefei, Anhui 230026, China

<sup>3</sup>Shanghai Branch, National Laboratory for Physical Sciences at Microscale and Department of Modern Physics, University of Science and Technology of China, Shanghai 201315, China

<sup>a)</sup>Electronic mail: [jiangx@ustc.edu.cn](mailto:jiangx@ustc.edu.cn)

## ABSTRACT

Current sources with extremely low noise are significant for many branches of scientific research, such as experiments of ultra-cold atoms, superconducting quantum computing, and precision measurements. Here we construct and characterize an analog-controlled bipolar current source with high bandwidth and ultra-low noise. A precise and stable resistor is connected in series with the output for current sensing. After being amplified with an instrumentation amplifier, the current sensing signal is compared with an ultra-low noise reference, and proportional-integral (PI) calculations are performed via a zero-drift low-noise operational amplifier. The result of the PI calculation is sent to the output power operational amplifier for closed-loop control of the output current. In this way, a current of up to 16 A can be sourced to or sunk from a load with a compliance voltage of greater than  $\pm 12$  V. The broadband current noise of our bipolar current source is about  $0.5 \mu\text{A}/\sqrt{\text{Hz}}$  and  $1/f$  corner frequency is less than 1 Hz. Applications of this current source in a cold atom interferometer, as well as active compensation of a stray magnetic field, are presented. A method for measuring high-frequency current noise in a 10 A DC current with a sensitivity down to a level of  $10 \mu\text{A}$  is also described.

Published under license by AIP Publishing. <https://doi.org/10.1063/1.5046484>

## I. INTRODUCTION

Current sources with low noise are widely used in laboratory applications.<sup>1-4</sup> Low-noise unipolar 200 mA current source for diode laser has been investigated by Libbrecht and Hall<sup>5</sup> and Durfee *et al.*<sup>6</sup> A source of bipolar current on the order of several amperes is used in nuclear magnetic resonance (NMR) experiments,<sup>7,8</sup> in which digital circuits are used for feedback and to control the current. These circuits use an analog-to-digital converter and a digital-to-analog converter with resolutions of up to 20 bits, which are complex and expensive. In cold-atom experiments, a magnetic field

produced by a precise coil current is used to control atoms. According to the Zeeman effect,<sup>9</sup> the energy levels of atoms are affected by a magnetic field, so the stability of the magnetic field is crucial for controlling atoms. To produce a stable magnetic field, low-noise current sources with a bandwidth of up to 3 kHz are used to cancel stray magnetic fields.<sup>10</sup> A current with relative stability on the order of  $10^{-5}$  is needed to produce a bias and a gradient magnetic field in the preparation of a single 2d quantum gas.<sup>11</sup> Analog control of the current source is needed, and so we can generate arbitrary waveforms that are needed in different experiments. Sine-wave and cosine-wave form currents at  $\omega_r = 2\pi * 1 \text{ kHz}$  are separately injected into

two pair of coils to create a rotating bias magnetic field for rapid rotation of the atomic dipoles in tuning of the magnetic dipole-dipole interaction within a dysprosium Bose-Einstein condensate.<sup>12</sup>

To meet the demands mentioned above, i.e., for a high bipolar current with low noise, an ultra-low noise analog-controlled bipolar current source with a maximum bandwidth of greater than 10 kHz is proposed and described in this article. We use a low-noise proportional-integral (PI) feedback part before the output stage and paralleled power operational amplifiers, OPA549, as the output stage for large bipolar current output. It can source and sink a DC current of up to 16 A (20 A in pulses), and the rise time when driving a 240  $\mu$ H coil from  $-1$  A to 1 A is less than 45  $\mu$ s (PI parameters optimized for high bandwidth). The broadband current noise of the bipolar current source is less than 0.5  $\mu$ A/ $\sqrt{\text{Hz}}$ , and the long-term noise is less than 10  $\mu$ A (rms, 0.01 Hz–10 Hz) over 100 s interval with 1/f corner frequency less than 1 Hz. A test method for measuring high-frequency noise down to 10  $\mu$ A level with a current of 10 A is also described. Adjustable P- and I-gains allow our current source to drive a variety of inductive loads without oscillations and large signal bandwidth ( $-1$  A to  $+1$  A for a 240  $\mu$ H inductive load) and be adjusted from

2 kHz to more than 10 kHz. We compare our current source BICUR with a commonly used current source of the High-Finesse BCS series using the same test method and BICUR exhibits better performance than the HighFinesse source in high-frequency, long-term tests and an atom interferometry application. Active compensation of a stray magnetic field in an experiment using BICUR is also presented, and the residual noise in the magnetic field after compensation is 23.3  $\mu$ G (rms, 2 Hz–3 kHz, 1  $\mu$ G =  $10^{-10}$  T), which is on the same level as the world's leading result.<sup>13</sup>

## II. CIRCUIT

As shown in Fig. 1, our circuit mainly consists of three parts: a PI calculation part, a power amplifier part, and a current sense part. The current through the load is sensed by the current sense part and converted to voltage. Then the voltage is feedback to the PI calculation part to perform PI calculations with the input voltage. The result calculated by the PI part is then sent to the power amplifier part, which has high driving ability to drive the inductive coil.

Current sources composed of operational amplifiers, such as the Howland Current Pump<sup>14</sup> can only source and sink

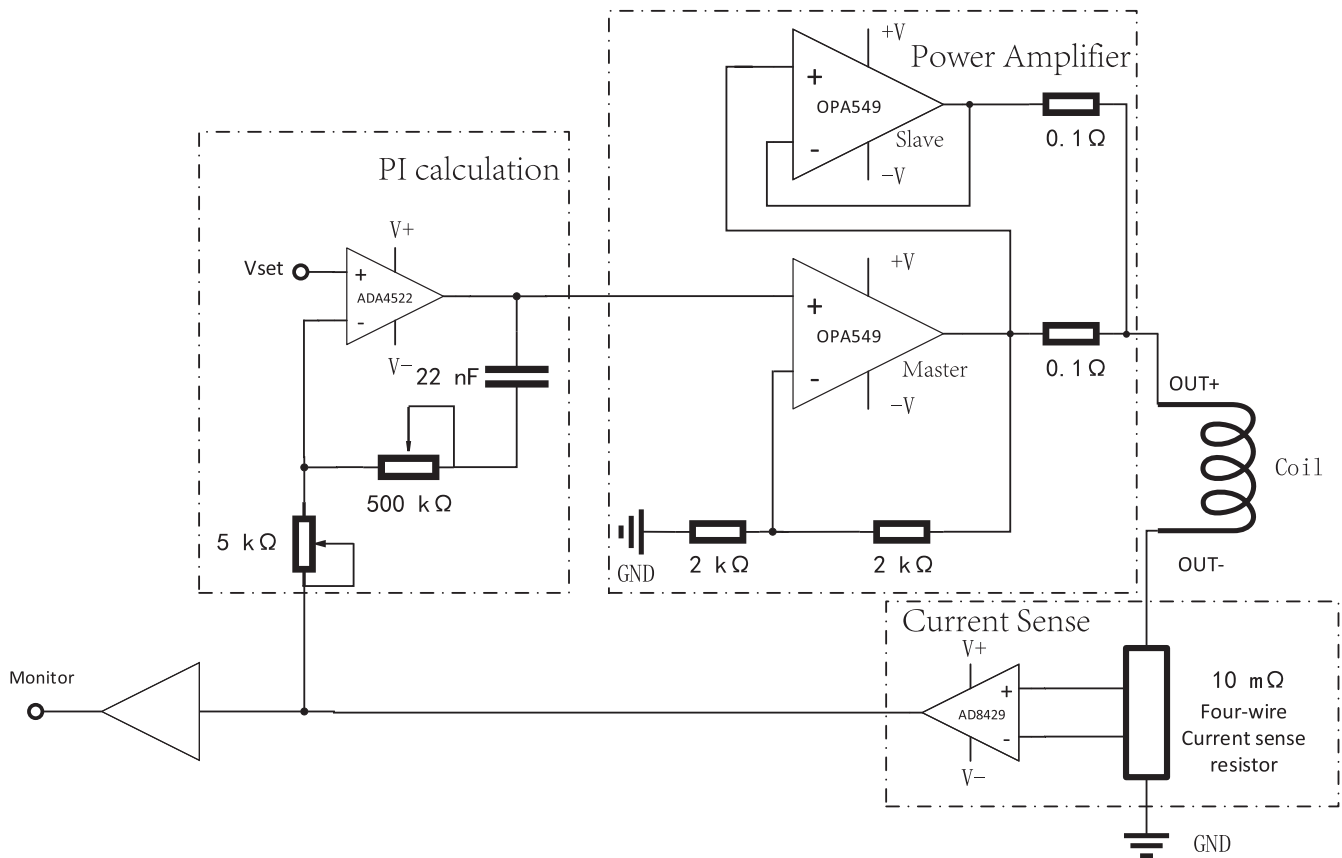


FIG. 1. Schematic of the bipolar current source.

currents of up to a few hundred milli-amperes. To obtain the capability for driving bipolar high current, we choose to use power operational amplifier OPA549 (Texas Instruments, Inc.), which can provide a current of up to 8 A (DC) and a pulse current of 10 A. The power supply rejection ratio of OPA549 is greater than 50 dB at 1 kHz, so the output current is less affected by noise of power supply than that in a discrete NPN/PNP bipolar junction transistor pair that we built. We connect the two OPA549s in parallel (one is master OPA549 and the other is slave OPA549 as shown in Fig. 1) to obtain the ability to drive a current of up to 16 A DC. The slave OPA549 is in a unity-gain configuration, and the positive input of slave OPA549 is connected to the output of master OPA549. To keep the output current of two OPA549s in balance, the output pins of both OPA549s are in series with a  $0.1 \Omega$  resistor respectively and then connected together. The feedback of the slave OPA549 makes the output voltage of the slave OPA549 to be the same as the master OPA549; hence, the current through two  $0.1 \Omega$  resistors are equal. If the output current of the master OPA549 rises, which means the output voltage of the master OPA549 rises, the output voltage of the slave OPA549 rises, so the output current of the slave OPA549 will rise; thus, the output currents of the two OPA549s are in balance. One may connect more OPA549s in parallel for higher current. Note that power consumption of OPA549s and the  $0.1 \Omega$  balance resistors is large, so we water cool them.

Input noise density of OPA549 at 1 kHz is  $70 \text{ nV}/\sqrt{\text{Hz}}$ , which is still higher than that of low-noise operational amplifiers. There is also large power consumption on the power operational amplifier which may lead to temperature change. So we use a PI calculation part before the power operational amplifier for current error detection and feedback regulation. By doing so, the noise is reduced and small temperature

change or drift affects the PI calculation part. As low frequency noise is also our consideration, we choose a zero-drift low-noise operational amplifier ADA4522 (Analog Devices, Inc.) to carry out the PI calculations, the input noise density of which is  $5.8 \text{ nV}/\sqrt{\text{Hz}}$  at 1 kHz. A resistor network and a capacitor are used with the ADA4522 amplifier to implement the PI calculations. As resistances affect the voltage division, we choose high stability VSMP series resistor (Vishay Precision Group) with a temperature coefficient of resistance (TCR) of  $0.05 \text{ ppm}/^\circ\text{C}$ . A polypropylene film capacitor is used as the integration capacitor owing to its low leakage current. The use of 1-gain and zero-drift op amp reduces the slow drift of the output current to a minimum level. Adjustable P- and I-gains allow our current source to drive a variety of inductive loads without oscillations. Note that PI parameters affect bandwidth, step response, and rms noise. The large signal bandwidth ( $-1 \text{ A}$  to  $+1 \text{ A}$  for a  $240 \mu\text{H}$  inductive load) can be adjusted from 2 kHz to more than 10 kHz by changing PI parameters. The broadband current noise is nearly the same in different PI parameters, so the noise is reduced when the bandwidth is limited. One can adjust PI parameters to limit the bandwidth to reduce rms noise or broaden the bandwidth to increase the step response speed.

The current sense part is crucial as its noise directly affects the feedback noise. In the region of our supply, i.e.,  $-20$  to  $+20 \text{ A}$ , a resistor provides the best solution for reliable operation.<sup>8</sup> We use four-wire metal strip resistor CSM3637Z (Vishay Precision Group) with a TCR of  $5 \text{ ppm}/^\circ\text{C}$  and a power rating up to  $3 \text{ W}$  to sense the current. The voltage of the sensed current is then amplified by an instrumentation amplifier because instrumentation amplifier has a high common-mode rejection ratio and lower noise than a current-sensing amplifier. An AD8429 amplifier (Analog Devices, Inc.) is chosen because its input noise density is only  $1 \text{ nV}/\sqrt{\text{Hz}}$  at 1 kHz. We

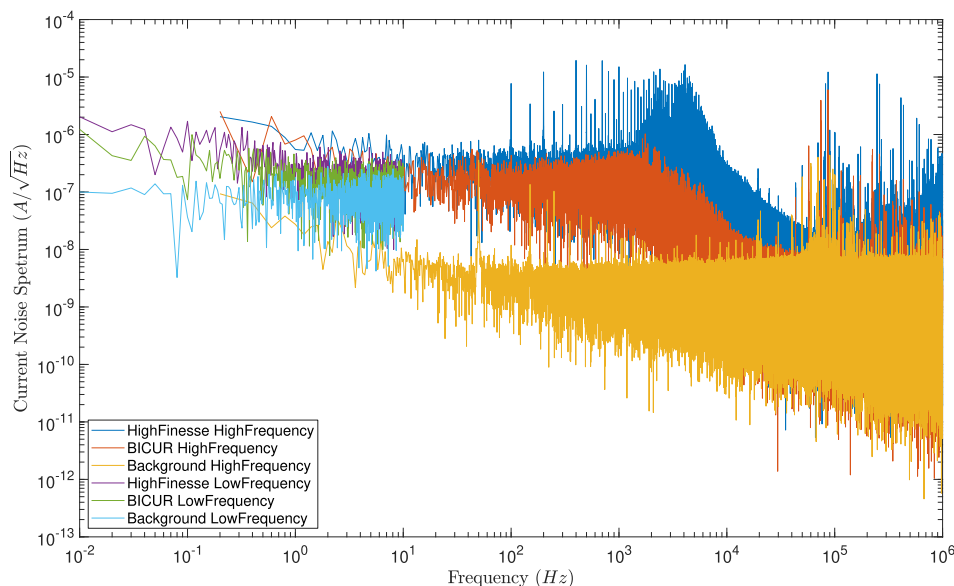


**FIG. 2.** High frequency noise and long-term stability (over 100 s with a 20/s sampling rate) of the bipolar current source. The high frequency noise rms of BICUR (red) is  $16.8 \mu\text{A}$  during 5 s test (rms, 0.2 Hz–300 kHz) whereas the rms value of the background noise (yellow) is  $4.1 \mu\text{A}$ , and the noise rms of a HighFinesse source (blue) is  $118 \mu\text{A}$ .

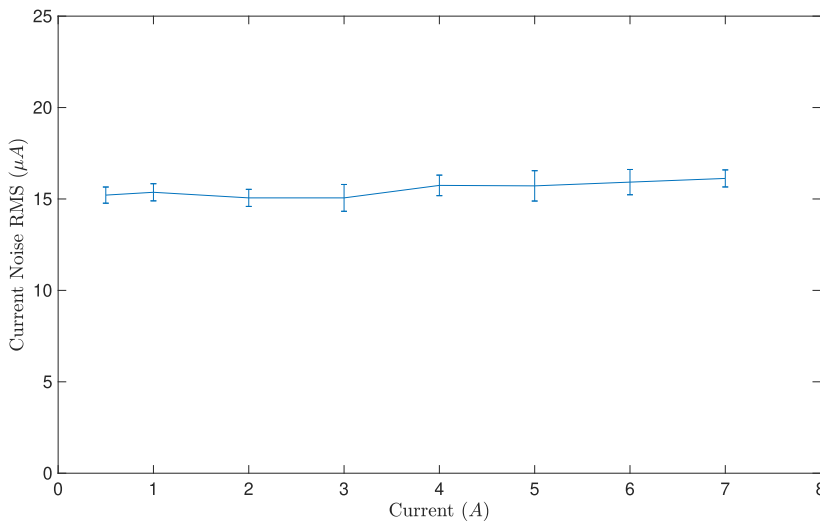


**FIG. 3.** High frequency current noise versus output current. The error bar is the standard deviation of 10 measurements for the test output current. The current noise does not change much when changing output current.

also use a VSMP series resistor as the gain set resistor for the AD8429 amplifier. A higher value current sense resistance is preferred because the current noise is converted to a higher voltage. The referred-to-input noise of AD8429 is relatively lower to the sensed voltage then, and the signal-to-noise ratio is increased. But as the current is high, we have to choose a resistance of as low as 10 mΩ to meet the power requirement of the current-sensing resistor. For small current applications, one can use a higher value resistance to reduce the current noise.

We use switching power supplies for the circuit because they are compact and light. The supply voltages are regulated by low-dropout linear regulators to reduce the noise. The input control voltage is either internal or external. The internal input control voltage is implemented with a potentiometer and voltage references.

### III. ELECTRICAL CHARACTERIZATION OF THE BIPOLAR CURRENT SOURCE

The measurement of noise on the order of 10 µA in a current on the order of 10 A is not easy, especially when high-frequency noise is taken into consideration. The maximum test current range of the 6½ digit multimeter 34411A (Keysight, formerly Agilent) that we have is only 3 A, and the resolution is only 1.5 ppm of the range with 0.02% rms noise adder of the range when the sampling rate is 1000/s. The maximum test current range of 8½ digit multimeter 3458A (Keysight, formerly Agilent) is only 1 A, and the sampling rate is 3/s [number of power line cycles (NPLC) = 10] when 7.5 digit accuracy is reached. The best current transducer we found is ITN 12-P made by LEM Danfysik, of which the test current range is 12.5 A and random noise is less than 10 ppm (rms) from 0 to 100 kHz. However fluxgate technology of this type cannot test

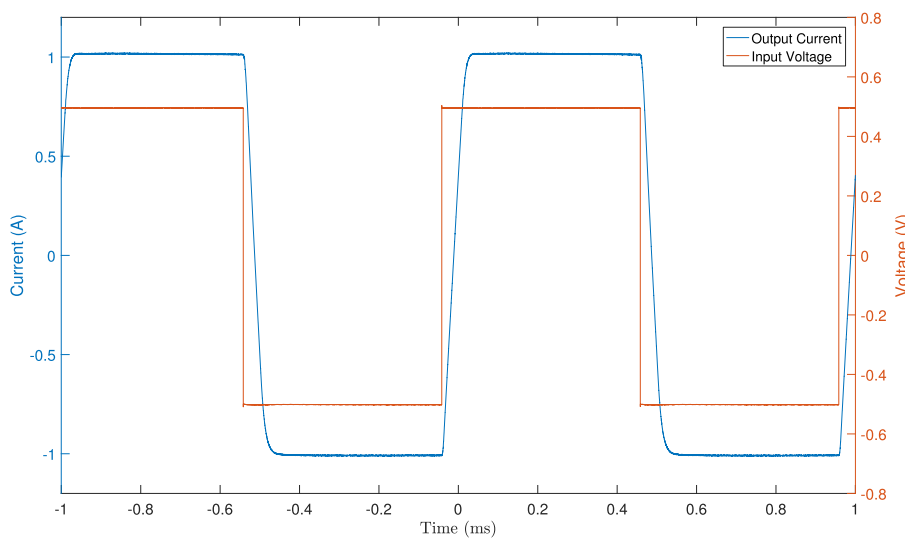


**FIG. 4.** Response of BICUR to a 1 kHz square wave (between -1 A and 1 A). The rise time (10%–90%) of the output current (blue) is 46.7 µs, whereas the fall time (90%–10%) is 43.45 µs.

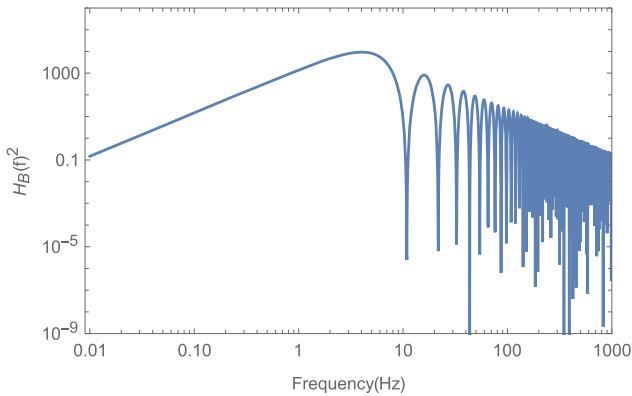


**FIG. 5.** Plot of transfer function  $H_B(\omega)^2$ , which has high values in the range from 0.5 Hz to 50 Hz, which implies that  $\delta_g$  is sensitive to magnetic noise in this range of frequencies.

small current noise on the order of  $10 \mu\text{A}$  for the flux through the transducer is easily affected by stray magnetic fields. The resistance of the current-sensing resistor in our circuit is only

$10 \text{ m}\Omega$ , and so though amplified by the instrumentation amplifier, the noise in the feedback signal for PI calculation is on the order of  $2 \mu\text{V}$  (assuming the current noise is  $10 \mu\text{A}$ ), which is hard to measure.

We use a  $1 \Omega$  non-inductive power resistor of which the power rating is  $300 \text{ W}$  to convert the current to voltage. The voltage is ac coupled and  $1000$  times amplified by a preamplifier, SR560 (Stanford Research Systems) and then measured by a 16-bit oscilloscope, PicoScope 4262 (pico Technology). We set the bandwidth of SR560 to  $0.1 \text{ Hz} - 300 \text{ kHz}$ . The bandwidth of PicoScope 4262 is  $3 \text{ MHz}$  over a range of  $\pm 10 \text{ mV}$ . To show the frequency component of  $100 \text{ Hz}$  noise clearly, we extend the measuring time to  $5 \text{ s}$  (sample rate:  $2 \text{ M/s}$ ) to have small FFT bin width. We compare our BICUR source with a HighFinesse BCS 5/10 source we have using the same test method. All the tests in Sec. III are with a  $240 \mu\text{H}$  coil as the load; here, the power resistor is in series with the coil. A typical result when the output current is  $4 \text{ A}$  is shown in Fig. 2. The broadband current noise of BICUR is less than  $0.5 \mu\text{A}/\sqrt{\text{Hz}}$ , the noise rms of BICUR is  $16.8 \mu\text{A}$  (low bandwidth PI parameters) during a  $5 \text{ s}$  test (rms,  $0.2 \text{ Hz} - 300 \text{ kHz}$ ) whereas the rms value of the background noise (power resistor left open,

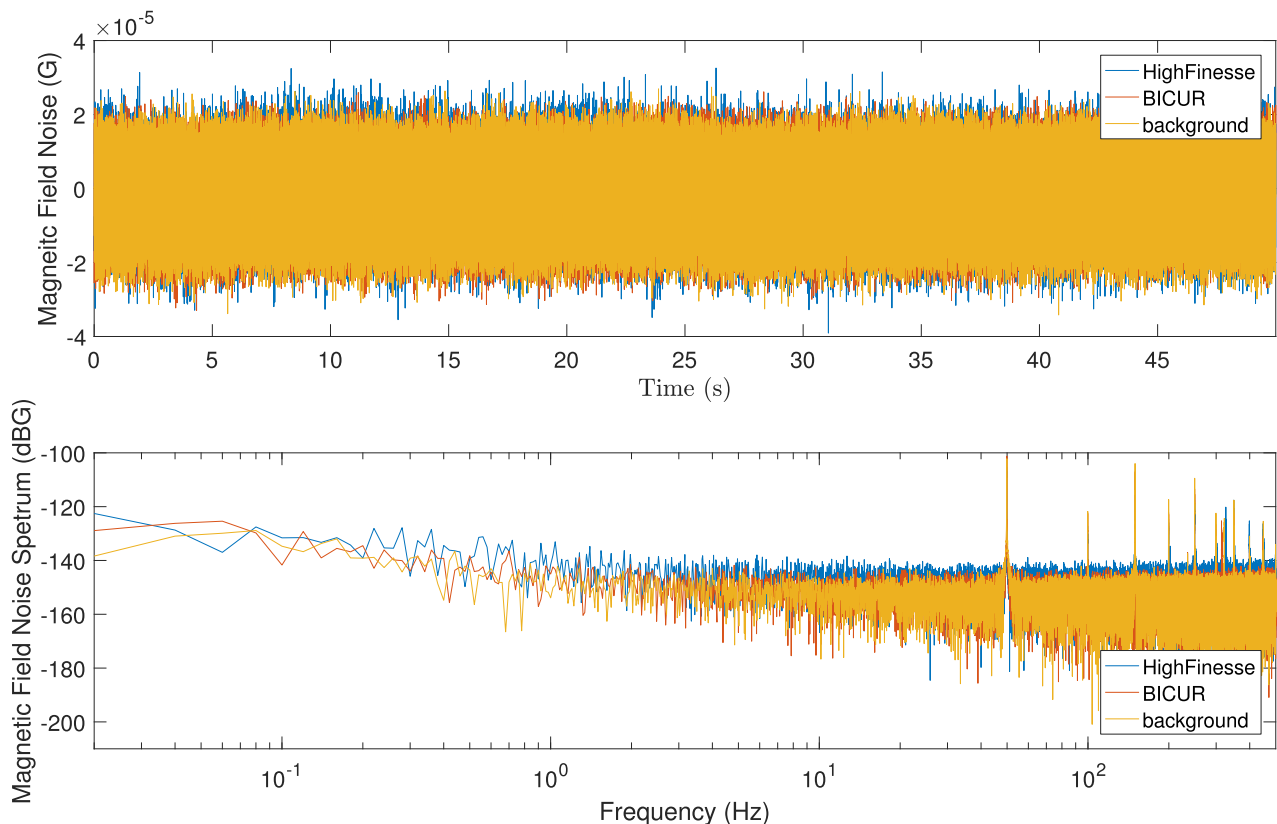


**FIG. 6.** Magnetic field measured inside a magnetic shield box (measurement period of  $50 \text{ s}$  with a  $1000/\text{s}$  sampling rate, average value subtracted). The magnetic noise rms when using BICUR (red) is  $10.4 \mu\text{G}$  (rms,  $0.02 \text{ Hz} - 500 \text{ Hz}$ ), whereas the rms value of the background magnetic noise (yellow) is  $10.7 \mu\text{G}$ , and the magnetic noise rms when using the HighFinesse source (blue) is  $10.8 \mu\text{G}$ . The calculated  $\delta_g$  values for the BICUR and HighFinesse sources are  $0.655 \mu\text{Gal}/\sqrt{\text{Hz}}$  and  $0.811 \mu\text{Gal}/\sqrt{\text{Hz}}$ , respectively.

no current flow through) is  $4.1 \mu\text{A}$ , and the noise rms of HighFinesse is  $118 \mu\text{A}$ . From the current noise spectrum, we can see that the HighFinesse source has higher noise than BICUR in the high frequency region. The result for the background noise indicates that we can measure high-frequency current noise at levels of as low as  $5 \mu\text{A}$  (rms, 0.2 Hz–300 kHz) in a 10 A current using this method. We also change the output current from 0.5 A to 7 A and measure the high frequency current noise. We can see from Fig. 3 that the current noise does not change much when changing output current. The errorbar is the standard deviation of 10 measurements for the test output current. The heat dissipation of our non-inductive power resistor is not good enough and it is hot when conducting 7 A current. So we did not measure current noise higher than 7 A. The broadband current noise remains the same when changing PI parameters, but since the bandwidth is wider for high-bandwidth situations than low-bandwidth, the rms noise when the bandwidth is set high is larger. The noise rms of BICUR is  $35.4 \mu\text{A}$  when the bandwidth is adjusted to 10 kHz, which is still much better than HighFinesse BCS 5/10 source.

To test the long-term stability, we use a 3458A multimeter (which is better than the 34411A model in terms of long term performance) in current measurement mode to measure the output current over a 100 s interval. As the maximum measurement range is 1 A, we set the output current to 0.8 A. To have low background noise, the NPLC is set to 1 with a sampling rate of 20/s. A typical result is also shown in Fig. 2, the average value is subtracted for better comparison of the results, the noise rms of BICUR is  $4.12 \mu\text{A}$  (0.01 Hz–10 Hz), whereas the rms value of the background noise (3458 A current input left open) is  $2.2 \mu\text{A}$ , and the noise rms of the HighFinesse source is  $6.15 \mu\text{A}$ . We can see from Fig. 2 that the high-frequency and low-frequency noise spectrum of BICUR meet at 10 Hz, which indicates the validity of our measurement. We can also see from the spectrums that the  $1/f$  corner frequency of BICUR is less than 1 Hz.

We input a 1 kHz square wave into BICUR to control the current between  $-1 \text{ A}$  and  $1 \text{ A}$  to demonstrate the drive capacity and bandwidth. A typical result with PI parameters optimized for high bandwidth is shown in Fig. 4, the load of which is a  $240 \mu\text{H}$  coil. The output current rise time (10%–90%) is  $46.7 \mu\text{s}$ , whereas the fall time (90%–10%) is  $43.45 \mu\text{s}$ . A greater change in the current will result in longer rise/fall times since for an inductive load, a fast changing current needs a high applied voltage. The voltage that we applied is  $\pm 15 \text{ V}$ . The maximum applied voltage for the OPA549 amplifier is  $\pm 30 \text{ V}$ , so the response time can be reduced by increasing the applied voltage, but the power consumption will increase in this case and more effective cooling will be needed.

#### IV. TEST IN OPERATIVE CONDITIONS

One of our applications comprises the generation of a bias magnetic field for an atom interferometry gravimeter which

is used to measure gravity. Noise in the bias magnetic field affects the results of gravity measurements in the following way:<sup>15</sup>

$$\delta_\phi^2 = \int_0^\infty H_B(\omega)^2 S_B(\omega) d\omega, \quad (1)$$

$$\delta_g = \frac{\delta_\phi}{|\vec{k}_{\text{eff}}| T^2 \sqrt{R}}, \quad (2)$$

where  $\delta_\phi$  is the phase noise,  $H_B(\omega)^2$  is a transfer function,  $S_B(\omega)$  is the power spectrum of the magnetic field,  $\omega$  is the angular frequency,  $\delta_g$  is the final noise in the gravity values, which reflects the quality of the gravity measurements,  $\vec{k}_{\text{eff}}$  is the effective wave vector of the Raman light,<sup>16</sup>  $T$  is the time between the interferometer pulses, and  $R$  is the repeat rate of gravity measurements. The transfer function  $H_B(\omega)^2$  is plotted in Fig. 5.

We can see that the transfer function  $H_B(\omega)^2$  has high values from 0.5 Hz to 50 Hz. So  $\delta_g$  is sensitive to magnetic noise in this range of frequencies.

The atom interferometry apparatus is inside a magnetic shield box. We put a magnetic sensor FL1-1000 (Stefan Mayer Instruments) into a magnetic shield box to measure the magnetic field inside the box. The ambient magnetic field mainly composed of the Earth's magnetic field is shielded to about 0.5 mG while the rms value of the AC component (rms, 0.02 Hz–500 Hz) is shielded to  $10.7 \mu\text{G}$  as shown in Fig. 6. The bias magnetic field is generated by injecting current into a pair

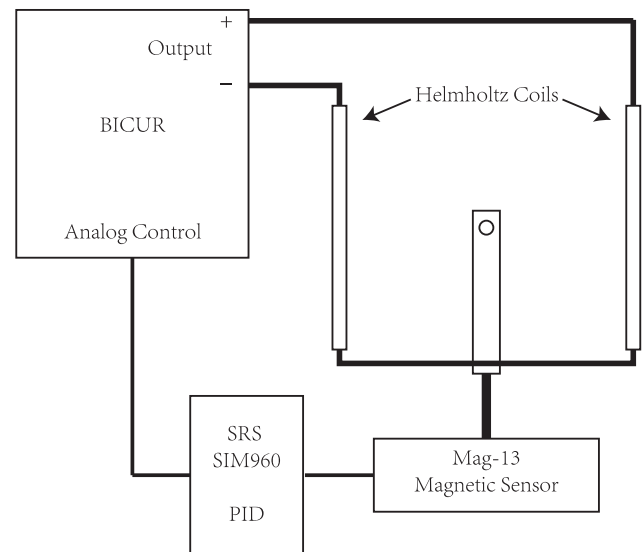


**FIG. 7.** Block diagram of magnetic compensation system. A magnetic field measured by a magnetic sensor is sent to a PID controller to perform PID calculations. BICUR controlled by PID calculated result drives Helmholtz coils to produce a magnetic field that actively compensates stray magnetic field noise.

of coils (inductance:  $35\ \mu\text{H}$ ) inside the magnetic shield box, so the noise in the current directly affects the bias magnetic noise. We use BICUR and HighFinesse BCS 2/25 to inject a 240 mA current into the bias coils to produce 200 mG magnetic field which is used in the experiment. The magnetic field is measured and shown in Fig. 6. We can see that the results for both the BICUR source and the HighFinesse source are close to the background values, while those for BICUR are a little better. The magnetic noise rms for BICUR is  $10.4\ \mu\text{G}$ , whereas the value for the HighFinesse source is  $10.8\ \mu\text{G}$ , which implies that the current noise (rms, 0.02 Hz–500 Hz) of the BICUR and HighFinesse sources is less than  $12\ \mu\text{A}$ . The  $\delta_g$  values for the BICUR and HighFinesse sources calculated using Eqs. (1) and (2) are  $0.655\ \mu\text{Gal}/\sqrt{\text{Hz}}$  ( $1\ \mu\text{Gal} = 10^{-8}\ \text{m/s}^2$ ) and  $0.811\ \mu\text{Gal}/\sqrt{\text{Hz}}$ , respectively. The  $\delta_g$  value for BICUR is better than that of the HighFinesse source because the magnetic noise for BICUR is lower in the sensitive frequency region.

BICUR can also be used to implement active compensation of a stray magnetic field. A block diagram of the magnetic compensation system is shown in Fig. 7, which is similar to the one used for active magnetic stabilization of the bias field in the work by Deans *et al.*<sup>17</sup> A magnetic sensor

Mag-13MSB100 (Bartington,  $-3\ \text{dB}$  Bandwidth: 3 kHz) is placed in the center of a pair of Helmholtz coils (inductance: 1.05 mH) to measure the magnetic field. The measured result is sent to an SIM960 proportional-integral-derivative (PID) controller (Stanford Research Systems) to perform PID calculations. The calculated result is then sent to control BICUR. The controlled BICUR drives the Helmholtz coils with a controlled current to produce a magnetic field that actively compensates stray magnetic field noise.

The magnetic field is measured by sampling the output of the Mag-13MSB100 sensor with a  $6\frac{1}{2}$  digit multimeter 34410A (Keysight, formerly Agilent) at a 10 000/s sampling rate and over a 0.5 s interval. The result of the magnetic compensation experiment is shown in Fig. 8. The rms value of the AC component (rms, 2 Hz–3 kHz, limited by Mag-13MSB100) of the background magnetic noise is  $125\ \mu\text{G}$  before compensation and is reduced to  $23.3\ \mu\text{G}$  with active compensation, which is on the same level as the result by Smith *et al.*<sup>13</sup> We can see from the noise spectrum that component of 50 Hz and its multiplication frequencies are significantly suppressed. In some applications, the magnetic sensor can be replaced with atomic magnetometer to get a better active compensation results.<sup>17-19</sup>

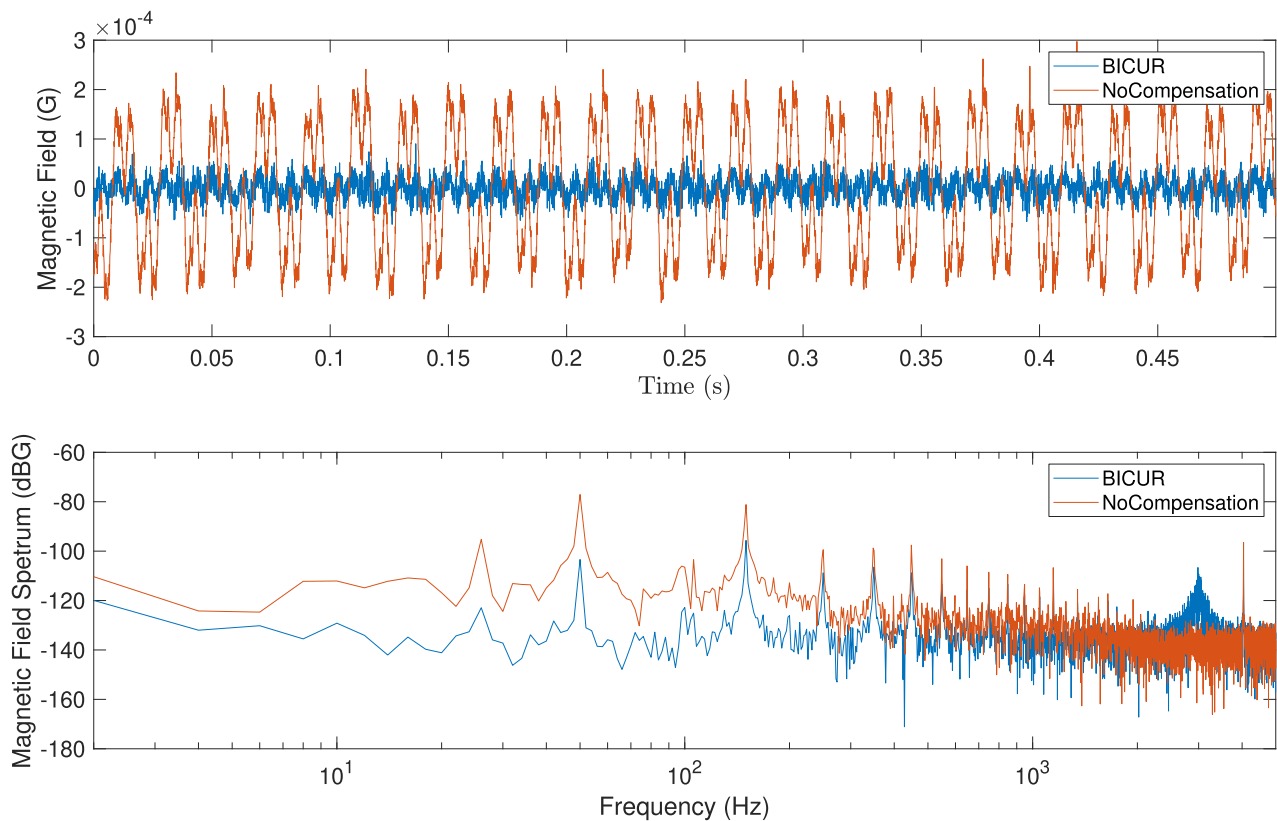


**FIG. 8.** Result of magnetic compensation experiment (measurement period of 0.5 s with 10 000/s sampling rate, average value subtracted). Background magnetic field noise rms is  $125\ \mu\text{G}$  (rms, 2 Hz–3 kHz) and is reduced to  $23.3\ \mu\text{G}$  via active compensation using BICUR.



## V. CONCLUSION

In summary, we have developed an analog-controlled low noise bipolar current source (BICUR) with a maximum bandwidth of greater than 10 kHz which is able to drive high-inductance coils. It can source and sink a current of up to 16 A (DC, 20 A in pulses), and the rise time when driving a 240  $\mu\text{H}$  coil from  $-1$  A to 1 A is less than 45  $\mu\text{s}$  (PI parameters optimized for high bandwidth). The broadband current noise of BICUR is less than  $0.5 \mu\text{A}/\sqrt{\text{Hz}}$  and the long-term noise is less than 10  $\mu\text{A}$  (rms, 0.01 Hz–10 Hz) over a period of 100 s with 1/f corner frequency less than 1 Hz. Adjustable P- and I-gains allow our current source to drive a variety of inductive loads without oscillations. It can be used in NMR, cold atom experiments, and for general purposes as well. The ultra-low current noise of BICUR enables the generation of stable magnetic fields, thus making the energy levels split by a magnetic field very stable, which is needed in many experiments. In an atom interferometry gravimeter experiment, the noise in gravity measurements  $\delta_g$  caused by a magnetic field generated using BICUR is  $0.655 \mu\text{Gal}/\sqrt{\text{Hz}}$ . The residual noise in the magnetic field after active compensation of stray magnetic fields using BICUR is 23.3  $\mu\text{G}$  (rms, 2 Hz–3 kHz).

## ACKNOWLEDGMENTS

The authors thank Yong-Guang Zheng and Bo Xiao for their help in the process of experimental measurements. This work was financially supported by the National Natural Science Foundation of China (Grant Nos. 61575185 and 11674301), the National Key R&D Program of China (Grant No. 2016YFA0301601), and the CAS Key Technology Talent Program. Special thanks to Professor Jian-Wei Pan for his guidance and insightful discussions.

## REFERENCES

- <sup>1</sup>V. Biancalana, G. Bevilacqua, P. Chessa, Y. Dancheva, R. Cecchi, and L. Stiacchini, *Rev. Sci. Instrum.* **88**, 035107 (2017).
- <sup>2</sup>S. Linzen, T. L. Robertson, T. Hime, B. L. T. Plourde, P. A. Reichardt, and J. Clarke, *Rev. Sci. Instrum.* **75**, 2541 (2004).
- <sup>3</sup>D. Talukdar, R. K. Chakraborty, S. Bose, and K. K. Bardhan, *Rev. Sci. Instrum.* **82**, 013906 (2011).
- <sup>4</sup>G. Scandurra, G. Cannatà, G. Giusi, and C. Ciofi, *Rev. Sci. Instrum.* **85**, 125109 (2014).
- <sup>5</sup>K. G. Libbrecht and J. L. Hall, *Rev. Sci. Instrum.* **64**, 2133 (1993).
- <sup>6</sup>C. J. Erickson, M. Van Zijll, G. Doermann, and D. S. Durfee, *Rev. Sci. Instrum.* **79**, 073107 (2008).
- <sup>7</sup>P. Skyba, *Rev. Sci. Instrum.* **62**, 2666 (1991).
- <sup>8</sup>J. Koivuniemi, R. Luusalo, and P. Hakonen, *Rev. Sci. Instrum.* **69**, 3418 (1998).
- <sup>9</sup>M. Fox, *Quantum Optics: An Introduction*, Oxford Master Series in Physics (OUP, Oxford, 2006).
- <sup>10</sup>C. J. Dedman, R. G. Dall, L. J. Byron, and A. G. Truscott, *Rev. Sci. Instrum.* **78**, 024703 (2007).
- <sup>11</sup>M. Endres, "Probing correlated quantum many-body systems at the single-particle level," Ph.D. thesis, Ludwig Maximilian University of Munich, Germany, 2014, available at [https://books.google.com/books?hl=zh-CN&lr=&id=aKrBBAAQBAJ&oi=fnd&pg=PR5&dq=Probing+correlated+quantum+many-body+systems+at+the+single-particle+level&ots=zc\\_A0-04qO&sig=K8CqXVmGDwELQsPVU5XKms61A8I#v=onepage&q=Probing%20correlated%20quantum%20many-body%20systems%20at%20the%20single-particle%20level&f=false](https://books.google.com/books?hl=zh-CN&lr=&id=aKrBBAAQBAJ&oi=fnd&pg=PR5&dq=Probing+correlated+quantum+many-body+systems+at+the+single-particle+level&ots=zc_A0-04qO&sig=K8CqXVmGDwELQsPVU5XKms61A8I#v=onepage&q=Probing%20correlated%20quantum%20many-body%20systems%20at%20the%20single-particle%20level&f=false).
- <sup>12</sup>Y. Tang, W. Kao, K.-Y. Li, and B. L. Lev, *Phys. Rev. Lett.* **120**, 230401 (2018).
- <sup>13</sup>A. Smith, B. E. Anderson, S. Chaudhury, and P. S. Jessen, *J. Phys. B: At., Mol. Opt. Phys.* **44**, 205002 (2011).
- <sup>14</sup>M. Murnane, AN-968 Current Sources: Options and Circuits, Analog Devices, Inc., 2008.
- <sup>15</sup>M.-K. Zhou, "Experimental demonstration of an atom interferometry gravimeter," Ph.D. thesis, Huazhong University of Science and Technology, Wuhan, 2011.
- <sup>16</sup>A. Peters, K. Y. Chung, and S. Chu, *Metrologia* **38**, 25 (2001).
- <sup>17</sup>C. Deans, L. Marmugi, and F. Renzoni, *Rev. Sci. Instrum.* **89**, 083111 (2018).
- <sup>18</sup>J. Fang and J. Qin, *Rev. Sci. Instrum.* **83**, 103104 (2012).
- <sup>19</sup>J. Belfi, G. Bevilacqua, V. Biancalana, R. Cecchi, Y. Dancheva, and L. Moi, *Rev. Sci. Instrum.* **81**, 065103 (2010).